Cell Reports, Volume *37*

Supplemental information

Alzheimer's vulnerable brain region relies on a distinct retromer core dedicated to endosomal recycling

Sabrina Simoes, Jia Guo, Luna Buitrago, Yasir H. Qureshi, Xinyang Feng, Milankumar Kothiya, Etty Cortes, Vivek Patel, Suvarnambiga Kannan, Young-Hyun Kim, Kyu-Tae Chang, Alzheimer's Disease Neuroimaging Initiative, S. Abid Hussaini, Herman Moreno, Gilbert Di Paolo, Olav M. Andersen, and Scott A. Small

SUPPLEMENTAL FIGURES AND TABLES

Figure S1

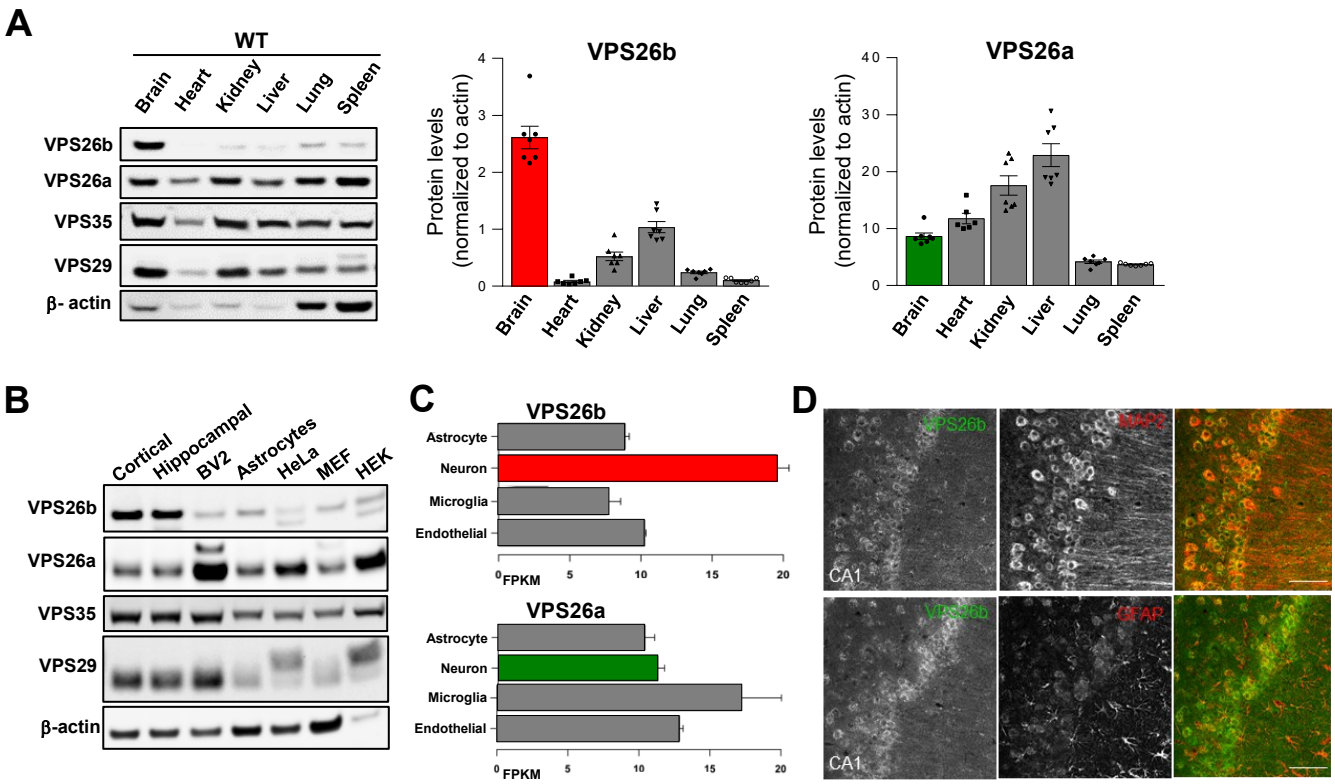

Figure S1. VPS26b is highly expressed in brain tissue and primary neurons. Related to Figure 1. (A) Expression levels of retromer proteins analyzed in a range of mouse tissue samples (n = 7), using β-actin as a loading control, show that while VPS26a is ubiquitously expressed among all tissues, VPS26b is highly expressed in the brain. **(B)** Western blot analysis of retromer proteins in different primary cultures, mouse and human cell lines, showing enrichment of VPS26b in primary neuronal cultures. **(C)** Bar diagram showing mRNA expression levels of VPS26b and VPS26a in astrocytes, neurons, microglia and endothelial cells. Data are from an RNA-sequencing transcriptome and splicing database reported by Zhang, Y. et al., 2014. RNA expression was measured in fragments per kilobase of transcript sequence per million mapped fragments (FPKM). (Reproduced with permission from http://Jiaqianwulab.org). **(D)** Representative confocal image of a 9 month old *WT* mouse brain section co-stained for VPS26b and the neuronal marker MAP2 (upper panel), or the GFAP astrocyte marker (lower panel). Note that VPS26b is present in neurons labeled for MAP2. Hippocampal CA1/subiculum regions are shown. Scale bar, 100μm.

Figure S2

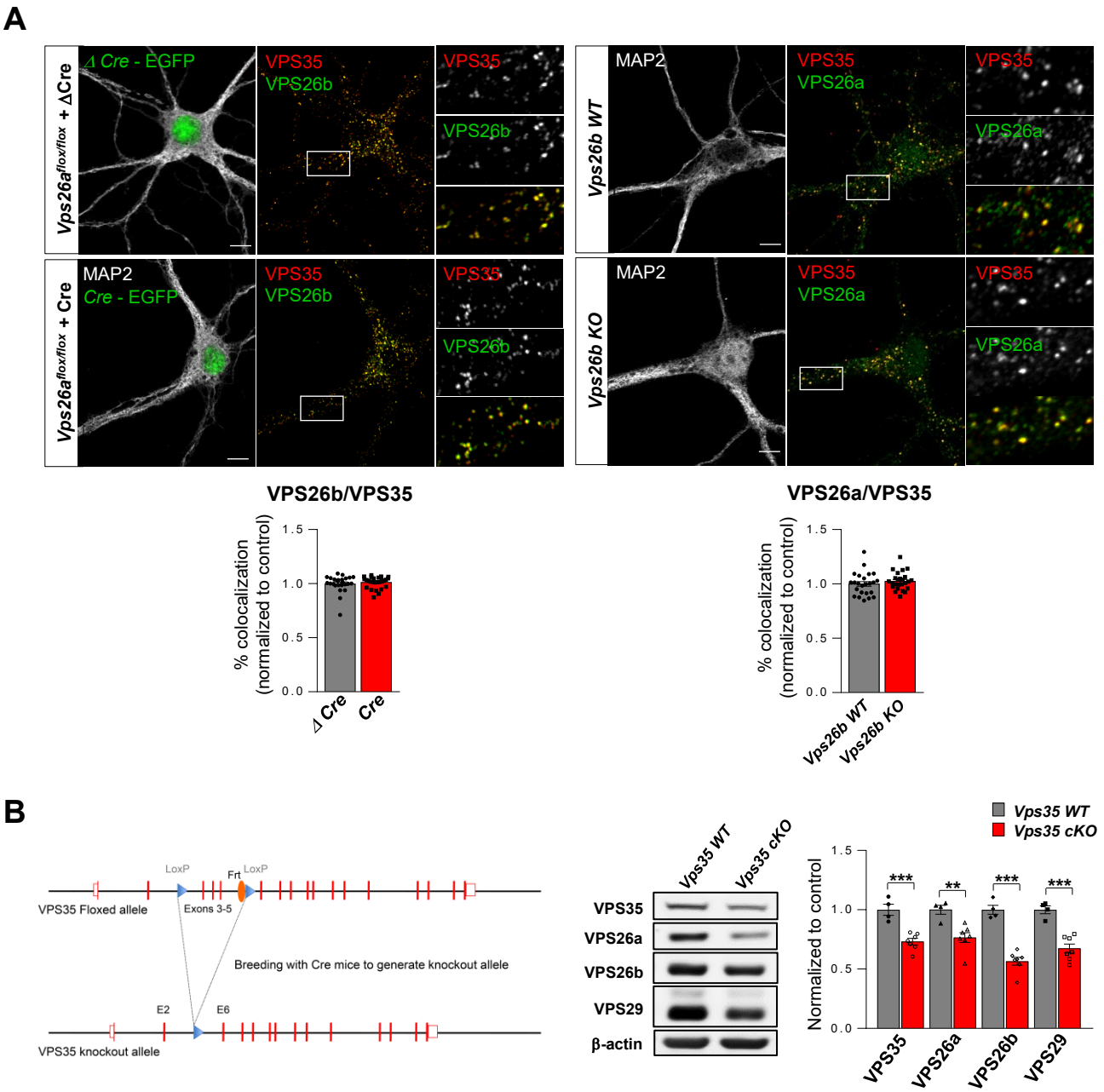

Figure S2. Distinct subcellular distribution of VPS26b and VPS26a in primary hippocampal neurons. Related to Figure 1. (A) Confocal images of hippocampal cultures derived from *Vps26a*$^{flox/flox}$ mice infected at DIV5 with lentiviruses expressing either an inactive Cre (Δ) or active (Cre) full-length Cre recombinase **(left panel)**. *Vps26b WT* and *Vps26b KO* hippocampal neurons were cultures for 15 days and analyzed by confocal microscopy **(right panel)**. Note both confocal analyses revealed that a complete deficiency of either VPS26 paralog have no secondary effect on the second core. VPS35 and VPS26 proteins are still observed in puncta structures reminiscent to early endosomes in both conditions. Pearson's correlation coefficient for VPS35 and each VPS26 paralog are unchanged in both deficiencies (*Vps26a*$^{flox/flox}$ + ΔCre *vs.* *Vps26a*$^{flox/flox}$ + Cre: $P = 0.4368$, in a non-parametric Mann-Whitney T-test; *Vps26b WT vs. Vps26b KO*: $P = 0.3477$, in unpaired two-sided student's *t*-test; n = 24-27 cells/condition, from three independent experiments). Scale bar, 10µm. **(B)** Neuronal-selective conditional *Vps35* knockout mice (*Vps35 cKO*) were generated by crossing mice expressing loxP-flanked *Vps35* (*Vps35*$^{flox/flox}$) with mice expressing Cre recombinase under the Camk2α promoter **(left panel)**. Western blots of hippocampus homogenates from *Vps35 cKO* (n = 4) and *Vps35 WT* littermates (n = 7). Quantitative western blot analysis revealed that a primary deficiency in VPS35 ($P = 0.0005$) results in a secondary reduction of all retromer core proteins including VPS26a ($P = 0.0045$), VPS26b ($P < 0.0001$) and VPS29 ($P = 0.0001$), arguing in favor of separate retromer cores **(right panel)**. Statistical analyses were performed using two-sided student's *t*-test. Bar graphs show means normalized levels, ± S.E.M., with *$P < 0.05$, **$P < 0.01$ and ***$P < 0.001$.

Figure S3

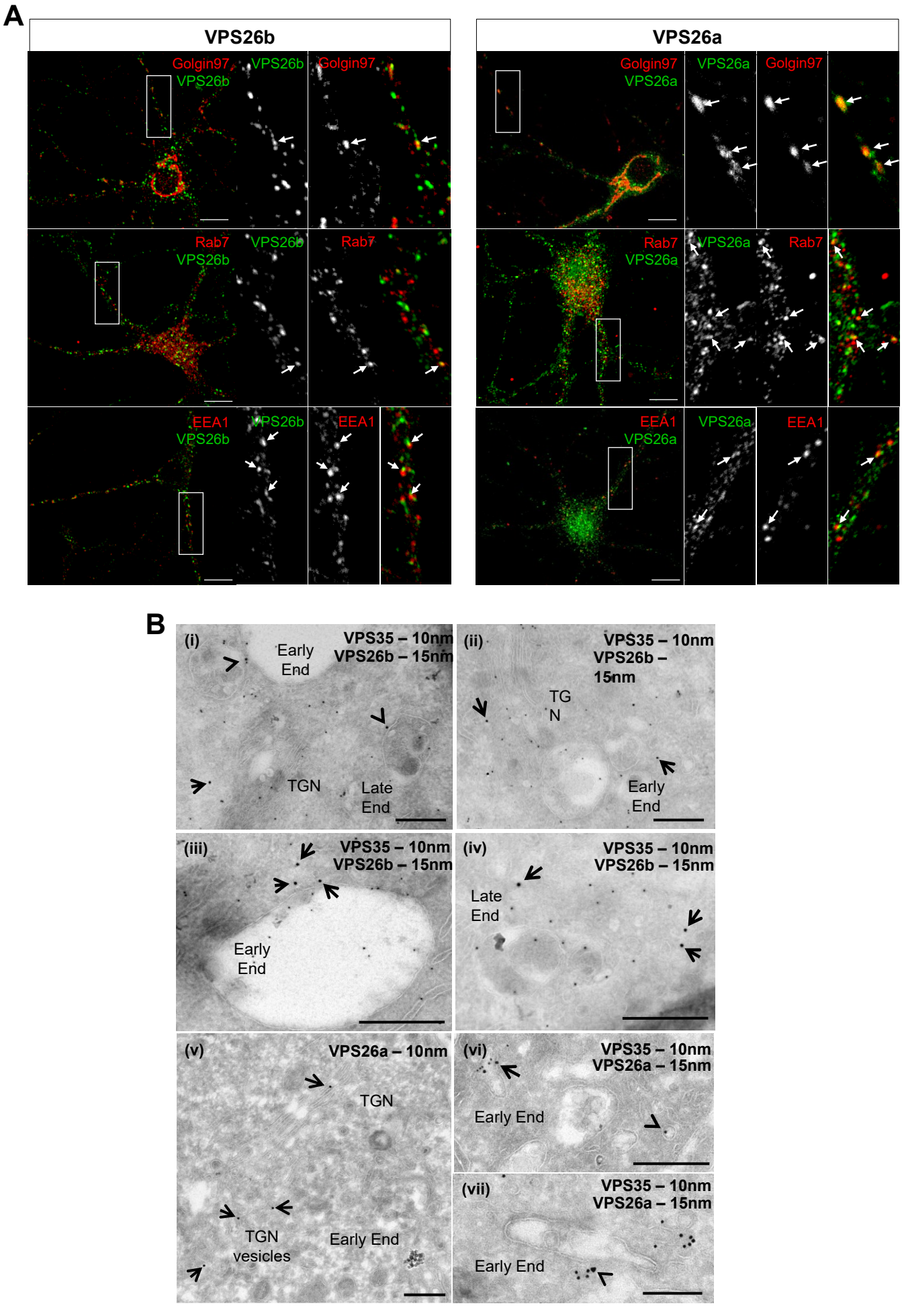
A
VPS26b
VPS26a
Golgin97
VPS26b
Golgin97
VPS26a
Rab7
VPS26b
Rab7
VPS26a
EEA1
VPS26b
EEA1
VPS26a
B
(i)
VPS35 – 10nm
VPS26b – 15nm
Early End
TGN
Late End
(ii)
VPS35 – 10nm
VPS26b – 15nm
TG N
Early End
(iii)
VPS35 – 10nm
VPS26b – 15nm
Early End
(iv)
VPS35 – 10nm
VPS26b – 15nm
Late End
(v)
VPS26a – 10nm
TGN
TGN vesicles
Early End
(vi)
VPS35 – 10nm
VPS26a – 15nm
Early End
(vii)
VPS35 – 10nm
VPS26a – 15nm
Early End

Figure S3. Distinct subcellular distribution of VPS26b and VPS26a in primary hippocampal neurons. Related to Figure 2. (A and B) Subcellular distribution of both VPS26 paralogs was performed using confocal and ultracryomicrotomy analysis. **(A)** Representative confocal images showing localization of VPS26 paralogs with different intracellular markers. Scale bar, 10µm. **(B)** Immunogold localization of VPS26b and VPS26a in ultrathin cryosections of hippocampal neurons. Sections were double immunogold labeled for VPS26b (PAG 15nm) and VPS35 (PAG 10nm) **(i-iv)** or for VPS26a (PAG 15nm) and VPS35 (PAG 10nm) **(vi-vii)**. Single immunogold labeling for VPS26a (PAG 10nm) is show in **(v)**. Note the presence of VPS26b in different endosomal compartments **(i)** (arrowheads) and tubules/vesicles in the vicinity of endosomes (**ii-iv**) (arrows). VPS26a is observed in the TGN **(v)** (arrows), early endosomes **(vi)** (arrow) and tubular-vesicular structures observed in close proximity to endosomes **(vi-vii)** (arrowheads). Scale bar, 250nm. TGN, *Trans*- Golgi Network; Early End, early endosomes; Late End, late endosomes.

Figure S4

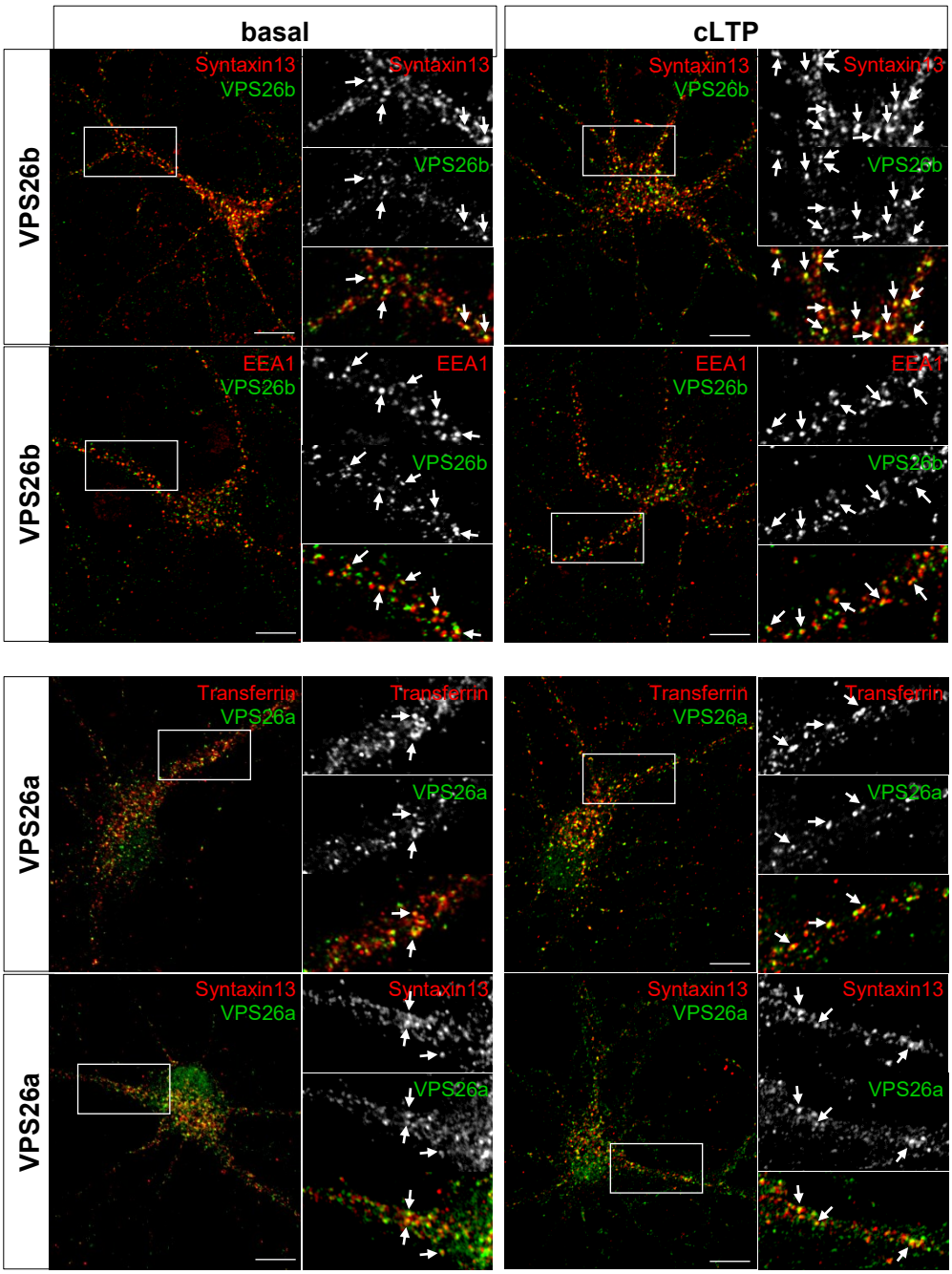

Figure S4. Chemical LTP results in a redistribution of VPS26 paralogs to different endosomal compartments. Related to Figure 2. Primary hippocampal neurons were stimulated with glycine for 5 minutes to induce cLTP and the subcellular distribution of VPS26b and VPS26a was assessed by confocal microscopy, using markers of early (EEA1) and recycling (Syntaxin13 and pulse-chase transferrin) endosomes. Regions outlined by white rectangles are shown at a higher magnification. Arrows highlight areas of colocalization. Note that cLTP stimulation greatly increases VPS26b localization to Syntaxin13 –positive recycling endosomes. Scale bar, 10µm.

Figure S5

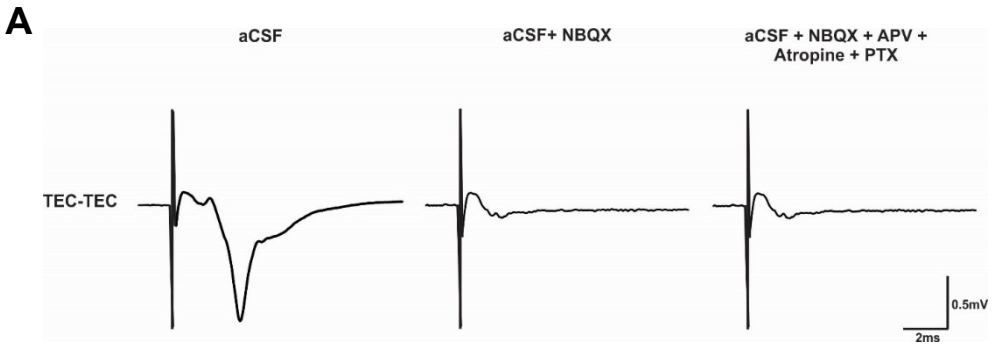
A
aCSF
aCSF+ NBQX
aCSF + NBQX + APV +
Atropine + PTX
TEC-TEC
0.5mV
2ms

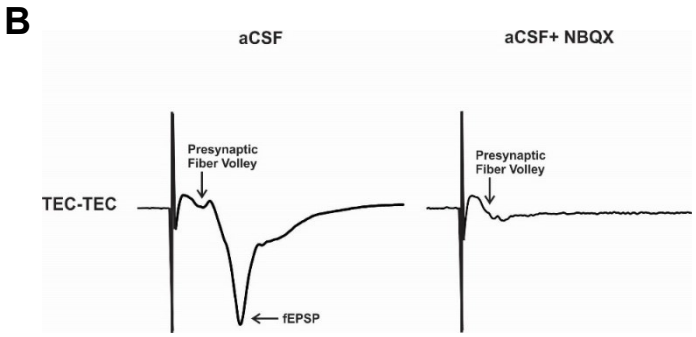
B
aCSF
aCSF+ NBQX
Presynaptic
Fiber Volley
Presynaptic
Fiber Volley
TEC-TEC
fEPSP

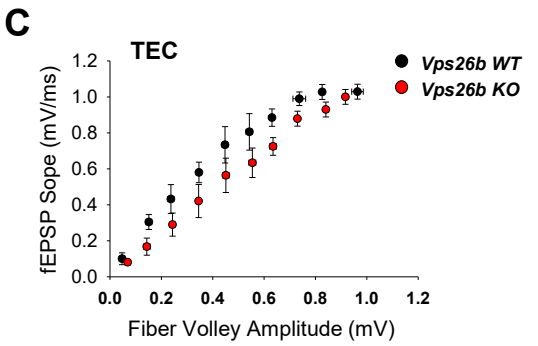
C
TEC
Vps26b WT
Vps26b KO
fEPSP Sope (mV/ms)
Fiber Volley Amplitude (mV)

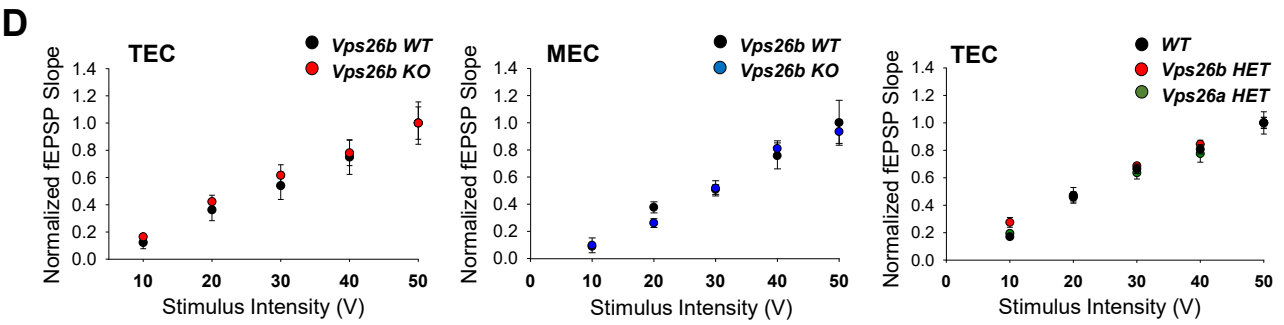
D
TEC
Vps26b WT
Vps26b KO
Normalized fEPSP Slope
Stimulus Intensity (V)
MEC
Vps26b WT
Vps26b KO
Normalized fEPSP Slope
Stimulus Intensity (V)
TEC
WT
Vps26b HET
Vps26a HET
Normalized fEPSP Slope
Stimulus Intensity (V)

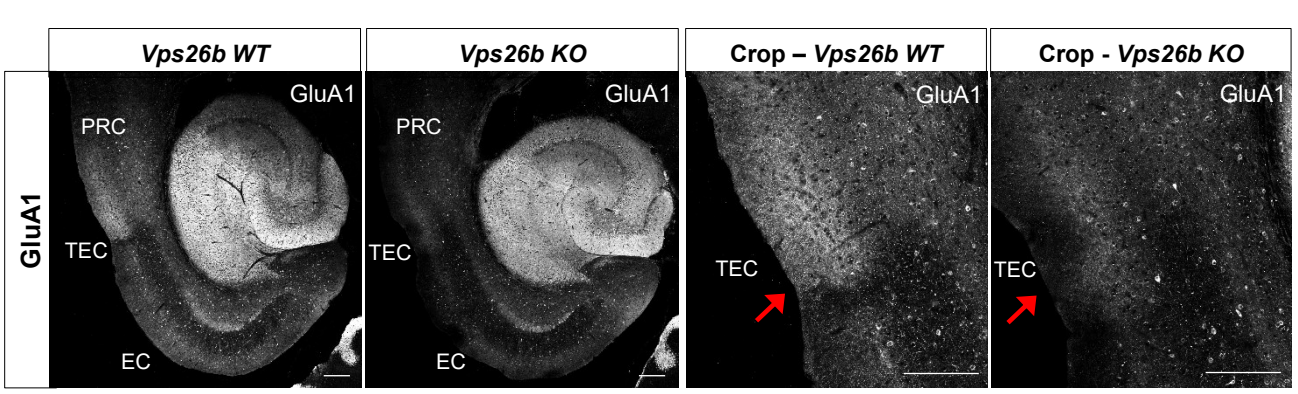
E
Vps26b WT
Vps26b KO
Crop – Vps26b WT
Crop - Vps26b KO
GluA1
PRC
TEC
EC

Figure S5. VPS26b deficient mice present normal basal synaptic transmission but reduced GluA1 levels in the TEC region. Related to Figure 3. (A) Example traces of the response evoked by electrical stimulation in the TEC region. n = 6 slices per genotype. aCSF **(left panel)**; aCSF + NBQX (10uM) **(middle panel)**; combined application of aCSF, NBQX, APV (30uM), Atropine (10 uM) and PTX (200uM) (**right panel**). **(B)** Representative traces of evoked fEPSP mediated by AMPA in the TEC region. Note that fEPSP, but not the fiber volley was abolished by NBQX. n = 6 slices per genotype. aCSF, artificial cerebral spinal fluid, NBQX, 2,3-dihydroxy-6-nitro-7-sulfamoyl-benzo[f]quinoxaline-2,3-dione; APV, (2R)-amino-5-phosphonovaleric acid; PTX, Picrotoxin. **(C)** Shown are the input-output curve of fEPSP slope normalized to fiber volley amplitude (mean ± SEM) in slices from *Vps26b WT* and *Vps26b KO* mice ($t_{(18)}$ = 0.82, P = 0.419, n = 6 slices per genotype). **(D)** Shown are the input-output relationship for all genotypes showing no significant changes in any of the input-output relationships of TEC or MEC in *Vps26b KO/HET* and *Vps26a HET* mice. **(E)** Focal reduction of GluA1 expression in the TEC of *Vps26b KO* mice. Representative confocal image of a 14 month old *Vps26b KO* mouse brain section and age-matched control immune-stained for GluA1. High-magnification images of superficial layers of TEC subregion are shown (bold red arrow). Scale bar, 200µm.

Figure S6

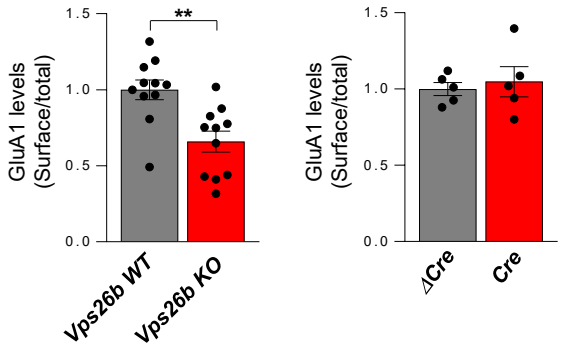

Figure S6: Only VPS26b depletion, but not VPS26a deficiency, results in a reduction of cell surface GluA1 levels. Related to Figure 4. Quantification of cell surface biotinylation experiments revealed a significant reduction in GluA1 surface levels in cells deficient for *Vps26b* compared to controls ($P = 0.001$), in a non-parametric Mann Whitney test. (n = 11 biological replicates, from 4 independent experiments). Note that VPS26a deficiency does not have any impact on GluA1 surface levels ($P = 0.6661$), in unpaired two-sided student's *t*-test. (n = 5 biological replicates, from 2 independent experiments). The ratio of surface to total GluA1 is shown. The *WT Vps26* ratios were set to 1, and all other values were calculated relative to it. Data expressed as mean ± S.E.M. *$P < 0.05$, **$P < 0.01$ and ***$P < 0.001$.

Figure S7

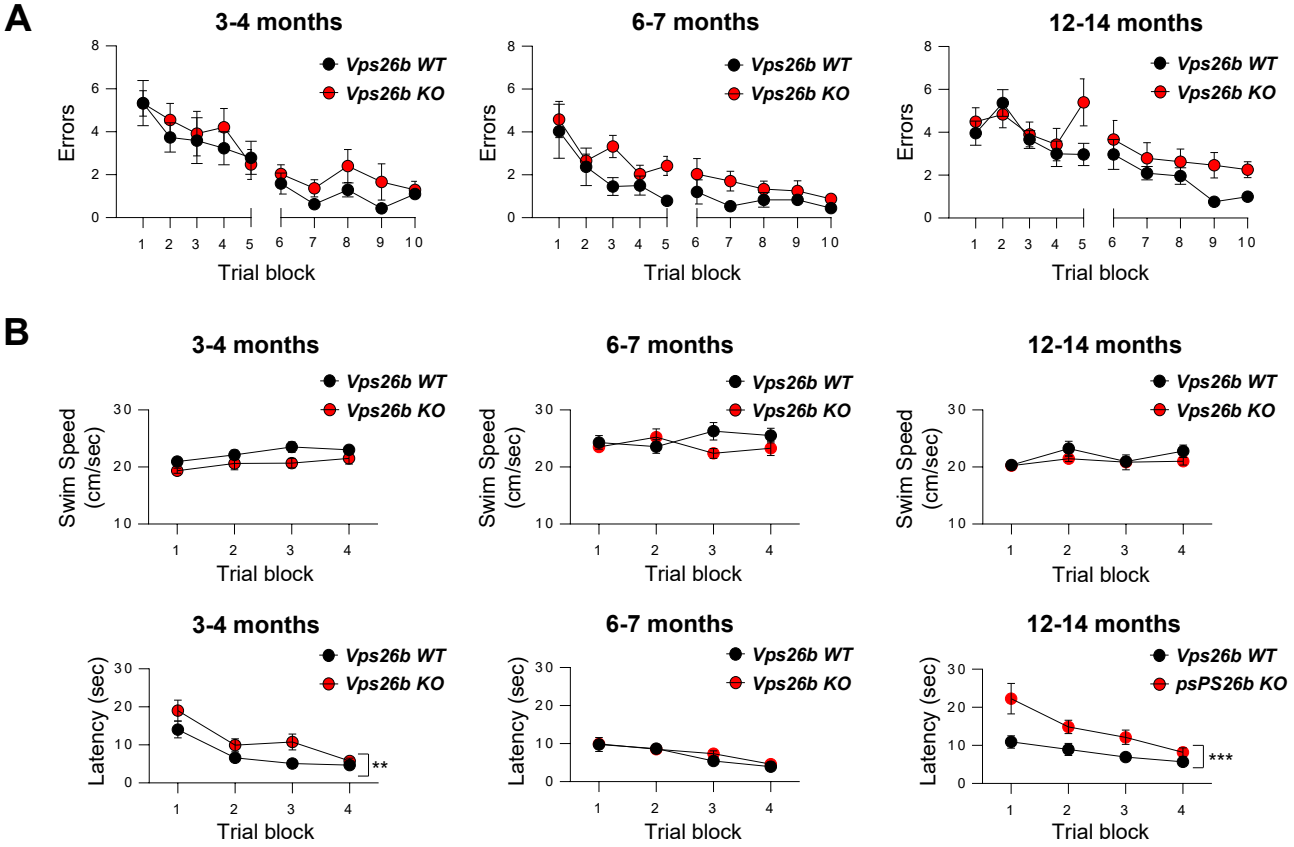

Figure S7. VPS26b deficient mice do not show hippocampal memory deficits compared to age-matched controls. **Related to Figure 5. (A)** Average number of errors committed (± S.E.M.) during each three-trial training block of a 2-days radial arm water maze task (RAWM), for the *Vps26b KO* mice and age-matched controls, at different time points: 3-4 months (*Vps26b WT*, n = 10; *Vps26b KO*, n = 9); 6-7 months (*Vps26b WT*, n = 8; *Vps26b KO*, n = 8) and 12-14 months (*Vps26b WT*, n = 10; *Vps26b KO*, n = 10). A two-way repeated-measures ANOVA with block and genotype as factors was used for data analysis. A trend for an hippocampal memory deficit is observed in older *Vps26b KO* mice compared to age-matched controls ($F_{(1,18)}$ = 3.516, P = 0.0771). **(B)** Animals tested on the 2-days RAWM were also tested in a visible platform to rule out impairments of vision, motivation, motor coordination, as well as cognitive deficits that are not restricted to spatial learning. Plots of the average escape latency and swim speed (± S.E.M.) for *Vps26b KO* mice and age-matched controls during training on a visible platform are shown. Two-way repeated –measures ANOVA with block and genotype as factors have identified a slight effect of genotype in latency at 3 and 12-14 months. Note that differences were noticed in the first trial blocks, by the last trial session, *Vps26b KO* mice took the same time to find the platform as their *WT* littermates. *P < 0.05, **P < 0.01 and ***P < 0.001.

Figure S8

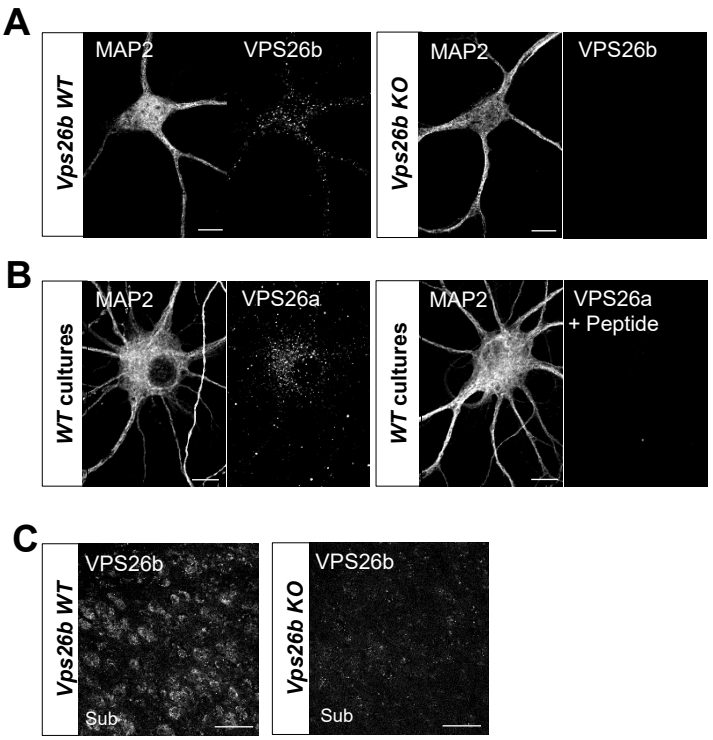

Figure S8. Validation of VPS26b and VPS26a reagents for Immunofluorescence techniques. Related to STAR Methods. (A) Immunocytochemistry analysis of *Vps26b WT* and *Vps26b KO* neuronal cultures showing VPS26b staining specificity. Scale bar, 10µm. **(B)** Immunofluorescence analysis of primary hippocampal cultures showing VPS26a staining specificity using a blocking peptide. Scale bar, 10µm. **(C)** Immunohistochemistry validation of VPS26b staining in brain tissue sections. Sub, subiculum. Scale bar, 50µm.

Supplemental Table S1

	AD (N=188)	Normal (N=169)
Age mean (std)	75.18 (7.50)	75.64 (5.18)
Gender M/F	99/89	83/86

Table S1. Demographic information of the human subjects used in the MRI analysis. Related to Figure 6. A total of 188 patients with AD and 169 normal subjects baseline scans were used in preparation of this article. The human MRI data was obtained from the Alzheimer's Disease Neuroimaging Initiative (ADNI) database (http://adni.loni.usc.edu).

Supplemental Table S2

Subject	SEX (F/M)	Age (yr)	PMI cold frozen (hr)	AD	Braak stage (NF tangles)	CERAD	NIAR
1	F	58	19.2	No	0*	B	Not el.
2	F	54	16.36	No	0*	Not el.	Not el.
3	M	36	8.37	No	0*	Not el.	Not el.
4	M	74	18.46	No	0*	Not el.	Not el.
5	M	75	36.17	No	0*	Not el.	Not el.
6	M	78	22.35	No	0*	Not el.	Not el.
7	F	89	14.15	No	0*	Not el.	Not el.
8	M	66	26.55	No	0*	Not el.	Not el.
9	F	79	20.1	No	0*	Not el.	Not el.
10	F	68	14.15	No	0*	Not el.	Not el.
11	M	85	21.03	No	0*	Not el.	Not el.
12	M	62	8.16	No	0*	Not el.	Not el.
13	F	89	6.2	No	0*	Not el.	Not el.
14	F	83	14.1	No	0*	Not el.	Not el.
15	F	83	9.15	No	0*	Not el.	Not el.
16	F	89	26.15	No	0*	Not el.	Not el.
17	F	89+	18.5	AD	5	B	High
18	F	79	31.25	AD	5	B	Intermediate
19	F	80	27.5	AD	6	C	High
20	F	66	9.45	AD	6	C	High
21	M	81	11.2	AD	3	B	Intermediate
22	F	83	23.5	AD	5	C	High
23	F	89	10.5	AD	5	C	Intermediate
24	M	86	23.08	AD	5	C	High

Table S2. Demographic information. Related to Figure 6. A total of 24 cases were used in this study: healthy controls, n = 16 and AD, n = 8. PMI, postmortem interval; AD, Alzheimer's disease; 0*, Minimal Tau pathology consistent with normal aging; Not el., Not eligible; CERAD, Consortium to Establish a Registry for Alzheimer's Disease; NIA-RI, National Institute on Aging–Reagan Institute.